

# Lawrence Berkeley National Laboratory

## LBL Publications

### Title

THE ENHANCEMENT OF CO HYDROGENATION ON RHODIUM BY TiO OVERLAYERS

### Permalink

<https://escholarship.org/uc/item/21g0v1z1>

### Author

Levin, M.E.

### Publication Date

1987-02-01

Center for Advanced Materials

# CAM

Submitted to Journal of Catalysis

## The Enhancement of CO Hydrogenation on Rhodium by $TiO_x$ Overlayers

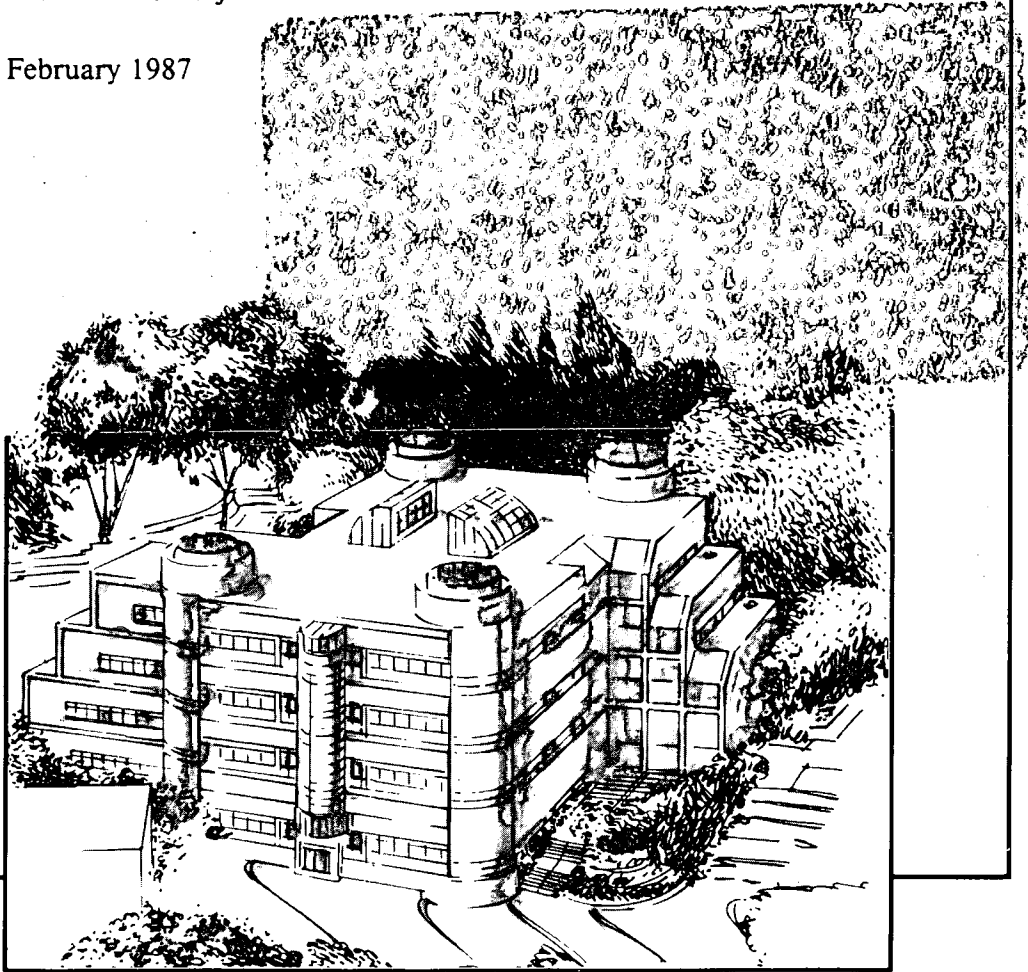
M.E. Levin, M. Salmeron, A.T. Bell,  
and G.A. Somorjai

February 1987

RECEIVED  
LAWRENCE  
BERKELEY LABORATORY

NOV 20 1987

LIBRARY AND  
DOCUMENTS SECTION



Materials and Chemical Sciences Division

Lawrence Berkeley Laboratory • University of California

ONE CYCLOTRON ROAD, BERKELEY, CA 94720 • (415) 486-4755

LBL-22812  
e-2

## **DISCLAIMER**

This document was prepared as an account of work sponsored by the United States Government. While this document is believed to contain correct information, neither the United States Government nor any agency thereof, nor the Regents of the University of California, nor any of their employees, makes any warranty, express or implied, or assumes any legal responsibility for the accuracy, completeness, or usefulness of any information, apparatus, product, or process disclosed, or represents that its use would not infringe privately owned rights. Reference herein to any specific commercial product, process, or service by its trade name, trademark, manufacturer, or otherwise, does not necessarily constitute or imply its endorsement, recommendation, or favoring by the United States Government or any agency thereof, or the Regents of the University of California. The views and opinions of authors expressed herein do not necessarily state or reflect those of the United States Government or any agency thereof or the Regents of the University of California.

LBL- 22812

The Enhancement of CO Hydrogenation on Rhodium by  $\text{TiO}_x$  Overlayers

by

<sup>1,4</sup>M.E. Levin, <sup>2</sup>M. Salmeron, <sup>1,2,4</sup>A.T. Bell\*, and <sup>1,2,3</sup>G.A. Somorjai

<sup>1</sup>Materials and Molecular Research Division and

<sup>2</sup>Center for Advanced Materials

Lawrence Berkeley Laboratory

and Departments of <sup>3</sup>Chemistry and <sup>4</sup>Chemical Engineering

University of California

Berkeley, CA 94720

Submitted to:

Journal of Catalysis

\*To Whom correspondence should be addressed

## ABSTRACT

The kinetics of CO hydrogenation at atmospheric pressure over a polycrystalline Rh foil with titania deposits were characterized with respect to the surface composition. The titania overlayers ( $\text{TiO}_x$ ,  $x \sim 1.9$ ) were prepared by titanium evaporation in ultra-high vacuum with subsequent oxidation. Coverages were determined by Auger electron spectroscopy (AES). A sharp maximum in methanation activity, relative to the clean Rh surface, was observed with coverage. A three-fold enhancement in activity was found for a  $\text{TiO}_x$  coverage of 0.15 ML. The increase in rate at low coverages was accompanied by a higher selectivity toward olefins (10%  $\rightarrow$  31%), a lower activation energy (24.4  $\rightarrow$  16.8 kcal/mole), a higher  $\text{H}_2$  reaction order (1.0  $\rightarrow$  2.6), and a higher CO reaction order (-1.0  $\rightarrow$  -0.3). The kinetic parameters for olefin production were noticeably different than those for paraffin production as well. The dependence of the activity on  $\text{TiO}_x$  coverage has been modeled through a Monte Carlo simulation assuming the existence of sites of high activity at the oxide/metal interface. This model is consistent with the premise of  $\text{Ti}^{3+}$  participation in the dissociation of CO.

## 1. INTRODUCTION

It has been established by various authors (see, for example, Refs. [1-4]) that the hydrogenation of CO over Group VIII metals supported on titania proceeds more rapidly than when these metals are supported on silica or alumina. A growing body of work [5-10] suggests that the higher activity of titania-supported catalysts is attributable to the migration of reduced titania ( $\text{TiO}_x$ ) species onto the surface of the supported metal particles. This view is further supported by recent evidence that the catalytic properties of  $\text{TiO}_2$ -promoted Pt-black, Pd/ $\text{SiO}_2$ , and Rh/ $\text{SiO}_2$  resemble those of  $\text{TiO}_2$ -supported Pt, Pd, and Rh [11-13].

To understand better the effects of  $\text{TiO}_x$  surface species overlayers, studies have been undertaken using metal foils and single crystals. Demmin *et al.* [14] observed an increase in the activity for CO hydrogenation when titania was deposited on a Pt foil, as well as a 10 kcal/mole decrease in the activation energy. Chung and co-workers [15] measured the reaction rate on a Ni(111) surface as a function of  $\text{TiO}_x$  coverage. They found a sharp maximum at 7.5% of a monolayer of  $\text{TiO}_x$  representing a five-fold increase in methanation activity. An increase in olefin formation in the presence of  $\text{TiO}_x$  was also observed.

The objective of the present study was to investigate the effects of  $\text{TiO}_x$  species on the activity and selectivity of CO hydrogenation over a Rh foil. Titania surface coverages of less than 0.30 ML were found to enhance significantly the rates of hydrocarbon formation, and, in particular, the synthesis of olefins. Investigations of the reaction kinetics revealed that, in addition,  $\text{TiO}_x$  surface species strongly influence the rate parameters associated with each product. A preliminary discussion of the data for methane formation is given in Ref. [16]. Reported here are the effects of  $\text{TiO}_x$  species on the kinetics of forming  $\text{C}_{2+}$  hydrocarbons. These results are discussed together with those for methane in the light of a proposed model for interpreting the effects of  $\text{TiO}_x$  promotion.

## 2. EXPERIMENTAL

A diffusion-pumped ultra-high vacuum (UHV) chamber with a base pressure of or below  $2 \times 10^{-9}$  torr was employed in this investigation. As described in our previous work [17], this chamber housed an Auger electron spectrometer, a quadrupole mass spectrometer, and an atmospheric pressure isolation cell. The isolation cell provided the capability of enclosing the sample and carrying out a reaction while the rest of the chamber remained in vacuum.

Titanium was vapor-deposited onto a clean Rh foil ( $1 \text{ cm}^2$ , 0.003 in. thickness, and 99.8% purity) by resistively heating a Ti-wrapped tungsten filament in a manner similar to the sample preparation in our chemisorption work [17]. The Rh foil was mounted on 0.030 in. Pt support wires. *In vacuo* oxidation ( $2 \times 10^{-6}$  torr  $\text{O}_2$  at 623 K) was found to be sufficient for oxidizing the Ti overlayer to near-stoichiometric  $\text{TiO}_x$ , where  $x \sim 1.9 \pm 0.15$ . Excess oxygen bound to the Rh was then removed as  $\text{CO}_2$  by repeated exposures to CO and heating to 773 K. The  $\text{TiO}_x$  coverage was monitored at three points on each face of the foil by Auger electron spectroscopy (AES) to ensure uniform deposition.

The monolayer coverage was determined from a plot of the normalized AES peak intensities for Rh, Ti, and O as a function of Ti dosing time [17]. The  $\text{TiO}_x$  overlayer grows in a two-dimensional manner until near-completion of the monolayer, followed by three-dimensional growth (*i.e.*, Stranski-Krastanov growth). Monolayer coverage for the  $\text{TiO}_x/\text{Rh}$  system occurs when the Rh signal is attenuated to 34% of its initial intensity. This value of the attenuation coefficient seems to indicate a bilayer structure of the titania.

The low surface area of the sample ( $2 \times 1 \text{ cm}^2$ ) necessitated operating reactions in a batch mode. The total reactor loop volume including the cell plus the circulation loop was  $125 \text{ cm}^3$ . Gases were circulated through the loop by a metal bellows pump at a rate of about  $200 \text{ cm}^3/\text{min}$ , as monitored with a rotameter.

A 6-port sampling valve with a  $0.25 \text{ cm}^3$  sampling loop permitted periodic re-

removal of a small portion of the reaction gas mixture for analysis. Hydrocarbons were separated and analyzed with a Hewlett-Packard Model 1920A Gas Chromatograph equipped with a flame ionization detector. A 6-ft column packed with Porapak N and held at 328 K easily separated all hydrocarbon products.

The reactions were performed at a total pressure of 1 atm. After passing through a cold trap to condense out metal carbonyls, carbon monoxide was introduced into the loop to a pressure of 0.33 atm. Hydrogen was passed through a liquid nitrogen trap and added to the loop to bring the total pressure to 1 atm. In the partial pressure dependence studies, where the sum of the H<sub>2</sub> and CO partial pressures was less than 1 atm, the total pressure in the loop was brought to 1 atm by filling with argon.

The reaction gas mixture was circulated for 20 min prior to a reaction with the catalyst remaining at room temperature. During this time, samples of the gas mixture were analyzed to determine if any hydrocarbons were initially present or if the reaction was already proceeding. A gas sample was taken 5 minutes after heating of the foil began and subsequent samples were taken at 10–15 minute intervals. After 1–2 hours of reaction, the foil was allowed to cool and no additional reactivity was observed. Following each reaction, the gas chromatograph was calibrated with a 1% CH<sub>4</sub>/Ar mixture. Reaction rates for each product were calculated from the initial slopes of product accumulation-versus-time plots. These rates remained constant during the first 30–40 minutes of each run before slowly decaying due to carbon build-up on the surface.

Evacuation of the reaction loop followed the completion of a reaction. This was accomplished with a rotary-vane mechanical pump followed by a sorption pump. When the reaction cell was adequately pumped, it was opened to the UHV chamber to allow sample characterization by AES.



### 3. RESULTS

Displayed in Fig. 1 is the methane production rate from CO and H<sub>2</sub> for varying TiO<sub>x</sub> coverages. Reaction rates were measured at a temperature of 553 K, and at H<sub>2</sub> and CO partial pressures of 0.67 atm and 0.33 atm, respectively. With the addition of small amounts of TiO<sub>x</sub> (<0.15 ML) to the clean Rh surface, a sharp rise in reaction rate is noted. At the maximum corresponding to 0.15 ML TiO<sub>x</sub>, a three-fold increase in rate is observed. Beyond this coverage, the rate decreases rapidly up to a coverage of about 0.30 ML and more slowly for higher TiO<sub>x</sub> coverages. The residual methanation activity at monolayer coverage could be reduced by increasing the TiO<sub>x</sub> coverage further. A gold foil mounted on the Pt support wires, in place of the Rh sample, showed negligible activity under identical reaction conditions indicating an insignificant contribution to the reaction rate by the support wires or reaction cell walls.

The effect of pre-reduction of the sample on the methanation rate was also investigated. Prior to reaction, the TiO<sub>x</sub>/Rh sample was heated in 50 torr H<sub>2</sub> at 753 K for 5 minutes. For five different titania coverages, hydrogen pretreatment was found to have no significant effect on the methanation rate.

More dramatic enhancements are observed in the formation of C<sub>2</sub> and C<sub>3</sub> hydrocarbons at low coverages as seen in Fig. 2. Most notable are the more than order-of-magnitude increases in rates for ethylene and propylene. As in the case of methane formation, the rates reach maxima around 0.15 ML TiO<sub>x</sub> and thereafter decrease rapidly with increasing titania coverage. Product selectivities are shown in Fig. 3. The methane content of the hydrocarbon product falls from a value of 94 mol% when no titania is present to nearly 60 mol% for  $\theta_{\text{TiO}_x} = 0.20$ . Ethylene and propylene are the predominant higher hydrocarbon species comprising roughly 34 mol% of the total hydrocarbon product. At higher coverages, the selectivities return to values more characteristic of clean Rh.

The influence of TiO<sub>x</sub> on the kinetic parameters (activation energy and reactant

partial pressure dependences) of CO hydrogenation on Rh was investigated for temperatures between 473 K and 633 K, H<sub>2</sub> partial pressures between 0.23 atm and 0.67 atm, and CO partial pressures between 0.037 atm and 0.33 atm. The observed rate of methane formation, R<sub>CH<sub>4</sub></sub>, was described with the power law expression given in Eqn. 1,

$$R_{\text{CH}_4} = k_0 \exp\left(-\frac{E_A}{RT}\right) p_{\text{H}_2}^n p_{\text{CO}}^m \quad (1)$$

where the temperature and partial pressures are represented by T, p<sub>H<sub>2</sub></sub>, p<sub>CO</sub>, respectively. The variations of the activation energy (E<sub>A</sub>), and the H<sub>2</sub> and CO partial pressure dependences (n and m, respectively) are shown in Figs. 4–6. The plot of activation energy versus coverage (Fig. 4) shows a minimum of 16.8 ± 0.5 kcal/mole at a coverage just above 0.2 ML. This represents a downward change of about 7.7 kcal/mole from the value of E<sub>A</sub> for clean Rh.

The hydrogen partial pressure dependence displayed in Fig. 5 rises sharply from a value of 1.0 ± 0.1 for clean Rh to 2.6 ± 0.1 at θ<sub>TiO<sub>2</sub></sub> = 0.10 and then slowly decays to a value of 1.5 near monolayer coverage. This trend is repeated in the CO partial pressure dependence plot (Fig. 6), but to a lesser extent. The CO order passes through a maximum at θ<sub>TiO<sub>2</sub></sub> = 0.15 with m = -0.3 ± 0.1, compared with -1.0 ± 0.1 for clean Rh.

The kinetic parameters for higher hydrocarbon formation were also determined with power-law expressions of the form of Eqn. 1 and the parameter values are plotted in Figs. 7–9. As in the case for methane, a decrease in the activation energy at low coverages is observed for ethane (Fig. 7) followed by a gradual rise in the activation energy above 0.30 ML. However, the presence of TiO<sub>2</sub> has virtually no effect on the activation energies of ethylene and propylene.

For all three hydrocarbons, the H<sub>2</sub> reaction orders increase significantly between 0 and 0.10 ML (Fig. 8). Ethane appears to follow the same trend as methane; the

olefins rise from near zero-order dependence to 1.5 order and fall slightly thereafter. The trends for the CO reaction orders are particularly interesting. Unlike methane, where a -1.0 order is observed, positive orders between 0.5 and 1.5 are seen for the other hydrocarbons on the clean surface (Fig. 9). With the addition of titania, the CO reaction orders for the C<sub>2+</sub> hydrocarbons decrease to -1.0. Propylene, though, exhibits a broad minimum at about 0.40 ML where the reaction becomes zero order in CO.

## 4. DISCUSSION

### 4.1 Methane Formation

As indicated in Fig. 1, a clear enhancement in methanation activity occurs for TiO<sub>x</sub> coverages under 0.30 ML while at higher coverages the rate diminishes gradually to a level well below that for clean Rh. Similar behavior has been observed by Chung *et al.* [15] for TiO<sub>x</sub> deposited on a Ni(111) surface and increases in activity of Pt foil [14], Pt-black [11], SiO<sub>2</sub>-supported Pd [12], and SiO<sub>2</sub>-supported Rh [13] have been reported upon promotion with TiO<sub>x</sub>.

It is apparent from Figs. 4-6 that at TiO<sub>x</sub> coverages comparable to those where R<sub>CH<sub>4</sub></sub> reaches a maximum, the value of E<sub>A</sub> is smaller, and the values of m and n are larger compared to the values of these parameters for clean Rh. A reduction in E<sub>A</sub> has also been reported by Demmin *et al.* [14] for a TiO<sub>x</sub>-promoted Pt foil and by Rieck and Bell [12] for TiO<sub>x</sub>-promoted Pd/SiO<sub>2</sub>. A sharp increase in hydrogen order was also observed by Vannice [18] for TiO<sub>2</sub>-supported Rh in comparison with Al<sub>2</sub>O<sub>3</sub>-supported Rh, while only a slight change in the CO partial pressure dependence was found.

The influence of TiO<sub>x</sub> on the CO hydrogenation activity of Group VIII metals has been attributed to Ti<sup>3+</sup> ions present at the perimeter of small TiO<sub>x</sub> islands decorating the metal surface [19-26]. For a TiO<sub>x</sub>-promoted Pt foil, Dwyer *et al.*

[27] detected a substantial concentration of  $\text{Ti}^{3+}$  species with x-ray photoelectron spectroscopy (XPS). XPS studies conducted in our own laboratory [28] have shown that the percentage of  $\text{Ti}^{3+}$  formed by either CO or  $\text{H}_2$  reduction increases with lower  $\text{TiO}_x$  coverage. Since the perimeter-to-area ratio of overlayer islands also rises with lower  $\text{TiO}_x$  coverages, these results suggest that Ti-O bonds near the periphery of  $\text{TiO}_x$  islands are more prone to attack by reducing agents chemisorbed on the Rh metal. The oxygen deficient  $\text{Ti}^{3+}$  species along the oxide island periphery may then interact with the oxygen end of CO adsorbed on near-by metal sites, as shown in Fig. 10. When CO is adsorbed on Rh sites adjacent to the Rh-Ti boundary, the C=O bond is long enough for the oxygen to reach the  $\text{Ti}^{3+}$  ion. The acid-base interaction between CO and the oxophilic  $\text{Ti}^{3+}$  should enhance the dissociation of CO—an essential step in the formation of methane.

To explain the observed methanation rate dependence on  $\text{TiO}_x$  coverage, we can propose that an ensemble of  $\text{Ti}^{3+}$  and Rh sites near the periphery of the islands are the active sites where an enhancement in rate occurs. The simplest ensemble that can be considered would include a single Rh site at the periphery. To determine the number of Rh atoms at the titania island periphery, we have employed a Monte Carlo simulation of  $\text{TiO}_x$  island growth around fixed nucleation sites. This simulation has been used to model the suppression in CO chemisorption at room temperature on  $\text{TiO}_x/\text{Rh}$  [17]. By excluding CO chemisorption at Rh sites bordering  $\text{TiO}_x$  islands, excellent agreement between the model and experimental data was found for a nucleation site density of  $4.5 \times 10^{13} \text{ cm}^{-2}$  ( $\sim 3\%$  site density). Calculations were performed for a  $100 \times 100$  hexagonal array.

With the nucleation site density determined from the chemisorption modeling, counting the number of these “peripheral” rhodium sites by use of the Monte Carlo simulation produces a function reaching a maximum at  $\theta_{\text{TiO}_x} \approx 0.35 \text{ ML}$ , corresponding to the maximum chemisorption suppression at low pressures [17]. Neither the position of the maximum nor the shape of the curve agree with the trend of the

experimental data.

A model which does give agreement with the observed trends is one in which a site pair consisting of a "peripheral" Rh site and an adjacent, non-"peripheral" Rh site has an intrinsically higher methanation activity. If it is assumed that the contribution of these peripheral site pairs to the total methanation rate is proportional to the product of the surface concentrations of each constituent site, then the total methanation rate in this model becomes [16]:

$$R_{\text{CH}_4} = S_{\text{T}} \left[ n_o r_o + \left( \frac{n_p}{n_{\text{T}}} \right) \left( \frac{n_{p'}}{n_{\text{T}}} \right) r_{pp'} \right] \quad (2)$$

where  $r_o$  and  $r_{pp'}$  represent the intrinsic methanation rates per unit catalyst area for the Rh sites unaffected by  $\text{TiO}_x$  and the highly active site pairs near the perimeter of the  $\text{TiO}_x$  islands, respectively. The numbers of each type of site present—exposed, "peripheral", adjacent to "peripheral", and the total—are given by  $n_o$ ,  $n_p$ ,  $n_{p'}$ , and  $n_{\text{T}}$ , respectively.

The number densities of the various types of site at various  $\text{TiO}_x$  coverages were determined through use of the Monte Carlo simulation. The values of  $n_o$ ,  $n_p$ , and  $n_{p'}$  were combined with the experimentally observed reaction rate for clean Rh,  $r_o$ , in Eqn. 2 to yield the total reaction rate as a function of coverage. The value of  $r_{pp'}$  was chosen so that the maximum value of the predicted rate agrees with the maximum in the observed methanation rate. For this condition to be met,  $r_{pp'}/r_o = 43$ . The dependence of the calculated rate on the  $\text{TiO}_x$  coverage, described by Eqn. 2, is shown in Fig. 11 (solid curve), along with the experimental points presented in Fig. 1, for comparison. Good agreement is seen between the location of the predicted rate maximum and that of the experimental data. The width of the calculated peak, though, is broader than that exhibited by the data.

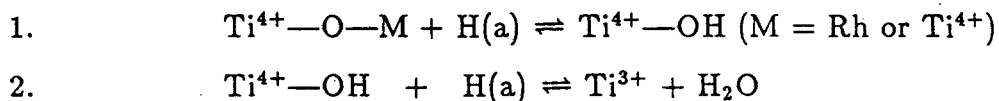
Another feature of this model is that it accounts for the extrema in kinetic parameters observed in Figs. 4–6. At low coverages ( $\leq 0.3$  ML), the rate is dominated

by the reaction occurring at the  $\text{TiO}_x/\text{Rh}$  interface, as reflected by the changes in activation energy and partial pressure dependences. At higher coverages, this contribution diminishes rapidly until kinetics typifying CO hydrogenation on clean Rh dominate.

At coverages approaching one monolayer, virtually all exposed, surface Rh atoms border  $\text{TiO}_x$  islands. These Rh sites may catalyze CO hydrogenation either through the mechanism normally occurring on Rh metal or through the  $\text{Ti}^{3+}$ -assisted pathway, depending on the prevalence of  $\text{Ti}^{3+}$  species at the metal/oxide interface under reaction conditions. The number of sites,  $n_o$ , catalyzing the reaction through the normal CO hydrogenation mechanism on bare Rh is therefore taken to be the total number of exposed Rh atoms.

In an earlier publication [16],  $n_o$  was taken as the number of Rh atoms that could chemisorb CO at low pressures. The plot of predicted rate versus  $\text{TiO}_x$  in this case is depicted by the dashed curve in Fig. 11. However, with  $n_o$  defined in this manner, the model does not predict the extrema in kinetic parameters of Figs. 4-6.

Through bonding with the oxygen in CO,  $\text{Ti}^{3+}$  is oxidized to the +4 oxidation state. Regeneration of the  $\text{Ti}^{3+}$  site must occur for this reaction pathway to be followed again. One scheme for the reduction of  $\text{Ti}^{4+}$  back to  $\text{Ti}^{3+}$  is given below



The high reaction order of 2.6 with respect to hydrogen in the  $\text{Ti}^{3+}$ -assisted reaction pathway suggests that five or six hydrogenation steps are crucial in determining the overall reaction rate; Reactions 1 and 2 comprise two of these steps. In contrast, for bare Rh, where CO dissociation is believed to be rate-determining, the first order  $\text{H}_2$  dependence suggests that only two hydrogenation steps are im-

portant. Consequently, changes in the abundance of hydrogen on the surface are expected to affect the  $Ti^{3+}$ -assisted methanation rate to a greater extent.

As higher  $TiO_x$  coverages are reached, there is a reduction in the number of exposed non-"peripheral" sites relative to the number of "peripheral" Rh sites. Furthermore, the high dispersion of the oxide overlayer serves to break up Rh-Rh pairs necessary for the chemisorption and dissociation of molecular hydrogen. The supply of surface hydrogen decreases rapidly with coverage and the impact on the  $Ti^{3+}$ -assisted reaction pathway, where the  $H_2$  partial pressure dependence is nearly cubic, is much greater than on the normal pathway, where the dependence is only linear. At the microscopic level, this means that at near-monolayer coverages, there is insufficient surface hydrogen to maintain the  $Ti^{3+}$ -assisted reaction rate and so the slower pathway, in which CO dissociation is rate-determining, is the principal contributant.

The absence of any effect from pre-reduction of the sample upon reaction rate, as observed in this study and others [20,29,30,31] may be related to the active role of  $Ti^{3+}$  species in CO hydrogenation. Whether pre-oxidized or pre-reduced, the oxidation state (and perhaps also the morphology) of the oxide overlayer may be determined by the reaction conditions, where both  $H_2$  and  $H_2O$  are present. In particular, the percentage of  $Ti^{3+}$  after reaction was found to be only weakly dependent on the pretreatment conditions [28].

#### 4.2 Formation of $C_{2+}$ Hydrocarbons

Comparison of Figs. 7-9 with Figs. 4-6 shows two principal patterns: (1) the kinetics of ethane formation are similar to those of methane formation and (2) the kinetics of ethylene and propylene formation are likewise similar. Significant differences are seen only in the case of the CO partial pressure dependence (e.g. -1.0 order for  $CH_4$  and +0.5 order for  $C_2H_4$ ) and these can be attributed to the requirement of additional surface carbon to form large hydrocarbons. Of particular

interest is the difference in hydrogen partial pressure dependences between paraffins and olefins. The methane and ethane hydrogen orders are between  $1/2$  and 1 greater than for ethylene and propylene. Similar behavior was noted by Dictor and Bell [32] for unsupported Fe and by Kellner and Bell [33] for  $\text{Al}_2\text{O}_3$ -supported Ru. In both of these studies, a difference in order of roughly  $1/2$  was seen between paraffins and olefins.

## 5. CONCLUSIONS

An enhancement in CO hydrogenation activity was observed upon deposition of  $\text{TiO}_x$  onto a polycrystalline Rh foil. The methanation rate passed through a maximum at 0.15 ML  $\text{TiO}_x$ , corresponding to a three-fold increase in rate, and was accompanied by maxima in the ethylene and propylene production rates. The activation energy and reactant partial pressure dependences also exhibited extrema at low  $\text{TiO}_x$  coverages while at high  $\text{TiO}_x$  coverages displayed behavior characteristic of bare Rh metal. The olefins exhibited different kinetic parameters than the paraffins. The modification of the catalytic properties of rhodium by titania has been attributed to participation by  $\text{Ti}^{3+}$  species at the metal/oxide interface in the CO dissociation step. A Monte Carlo simulation gives good quantitative agreement between the experimental data and a model invoking two-site ensembles along the  $\text{TiO}_x$  island periphery.

## ACKNOWLEDGEMENTS

We are grateful to Kevin J. Williams and Howard Chu for their assistance in performing experiments. This work was supported by the Office of Basic Energy Sciences, Chemical Sciences Division of the US Department of Energy under Contract DE-AC03-76SF00098.



## REFERENCES

1. Bell, A.T., "Supports and Metal-Support Interactions in Catalyst Design" in "Catalyst Design—Progress and Perspectives" (L.L. Hegedus, Editor), Wiley, New York, 1987.
2. Katzer, J.R., Sleight, A.W., Gajardo, P., Michel, J.B., Gleason, E.F., and McMillan, S., *Faraday Discuss.* **72**, 121 (1981).
3. Orita, H., Naito, S., Tamaru, K., *J. Chem. Soc., Chem. Commun.* **18**, 993 (1983).
4. Haller, G.L., Henrich, V.E., McMillan, M., Resasco, D.E., Sadeghi, H.R., and Sakellson, S., in "Proceedings, 8th International Congress on Catalysis," Vol. V, p. 135. Berlin, 1984.
5. Santos, J., Phillips, J., and Dumesic, J.A., *J. Catal.* **81**, 147 (1983).
6. Resasco, D.E., and Haller, G.L., *J. Catal.* **82**, 279 (1983).
7. Sadeghi, H.R., and Henrich, V.E., *J. Catal.* **87**, 279 (1984).
8. Takatani, S., and Chung, Y.-W., *J. Catal.* **90**, 75 (1984).
9. Belton, D.N., Sun, Y.-M., and White, J.M., *J. Phys. Chem.* **88**, 5172 (1984).
10. Baker, R.T.K., Chludzinski, J.J., and Dumesic, J.A., *J. Catal.* **93**, 312 (1985).
11. Dwyer, D.J., Robbins, J.L., Cameron, S.D., Dudash, N., and Hardenbergh, J., *ACS Symposium Ser.* No. 298, "Strong Metal Support Interaction" (R.T.K. Baker, S.J. Tauster, and J.A. Dumesic, Eds.), p. 21, 1986.
12. Rieck, J.S., and Bell, A.T., *J. Catal.*, 1986, in press.
13. Pande, N.K., Ph.D. Thesis, University of California, Berkeley, CA.
14. Demmin, R.A., Ko, C.S., and Gorte, R.J., *J. Phys. Chem.* **89**, 1151 (1985).
15. Chung, Y.-W., Xiong, G., and Kao, C.-C. *J. Catal.* **85**, 237 (1984).
16. Levin, M.E., Salmeron, M., Bell, A.T., and Somorjai, G.A., *Faraday Symp. Chem. Soc.* **21**, paper 10 (1986).
17. Levin, M., Salmeron, M., Bell, A.T., and Somorjai, G.A., *Surf. Sci.* **169**,

123 (1986).

18. Vannice, M.A., *J. Catal.* **74**, 199 (1982).
19. Burch, R., and Flambard, A.R., *J. Catal.* **78**, 389 (1982).
20. Bracey, J.D., and Burch, R., *J. Catal.* **86**, 384 (1984).
21. Anderson, J.B.F., Bracey, J.D., Burch, R., and Flambard, A.R., in "Proceedings, 8th International Congress on Catalysis," Vol. V, p. 111. Berlin, 1984.
22. Vannice, M.A., and Sudhakar, C., *J. Phys. Chem.* **88**, 2429 (1984).
23. Sudhakar, C., and Vannice, M.A., *J. Catal.*, **95**, 227 (1985).
24. Sachtler, W.M.H., in "Proceedings, 8th International Congress on Catalysis," Vol. V, p. 151. Berlin, 1984.
25. Sachtler, W.M.H., Shriver, D.F., Hollenberg, W.B., and Long, A.F., *J. Catal.*, **92**, 429 (1985).
26. Rieck, J.S. and Bell, A.T., *J. Catal.*, **96**, 88 (1985).
27. Dwyer, D.J., Cameron, S.D., and Gland, J., *Surf. Sci.* **159**, 430 (1985).
28. Levin, M.E., Salmeron, M., Bell, A.T., and Somorjai, G.A., results to be published.
29. Solymosi, F., Tombácz, I., and Kocsis, M., *J. Catal.* **75**, 78 (1982).
30. Vannice, M.A., Twu, C.C., and Moon, S.H., *J. Catal.* **82**, 213 (1983).
31. Morris, S.R., Moyes, R.B., and Wells, P.B., in "Studies in Surface Science and Catalysis" (B. Imelik *et al.*, Eds.), Vol. 11, p. 247, Elsevier, Amsterdam, 1982.
32. Dictor, R.A., and Bell, A.T., *Applied Catalysis* **20**, 145 (1986).
33. Kellner, C.S., and Bell, A.T., *J. Catal.* **70**, 418 (1981).

## FIGURE CAPTIONS

Figure 1: Methanation rate on  $\text{TiO}_x/\text{Rh}$  as a function of  $\text{TiO}_x$  coverage. Reaction conditions were: 553 K, 1 atm total pressure, and a  $\text{H}_2:\text{CO}$  ratio of 2:1.

Figure 2: Higher hydrocarbon formation rates on  $\text{TiO}_x/\text{Rh}$  as a function of  $\text{TiO}_x$  coverage. Reaction conditions were: 553 K, 1 atm total pressure and a  $\text{H}_2:\text{CO}$  ratio of 2:1.

Figure 3: Hydrocarbon product selectivity as a function of  $\text{TiO}_x$  coverage.

Figure 4: Activation energy for methane formation as a function of  $\text{TiO}_x$  coverage. Reaction conditions identical to Fig. 1 except the temperature was varied between 473 and 633 K.

Figure 5: Hydrogen partial pressure dependence as a function of  $\text{TiO}_x$  coverage. Reaction conditions identical to Fig. 1 except the hydrogen partial pressure was varied from 0.23 to 0.67 atm.

Figure 6: CO partial pressure dependence as a function of  $\text{TiO}_x$  coverage. Reaction conditions identical to Fig. 1 except the CO partial pressure was varied between 0.037 and 0.33 atm.

Figure 7: Activation energy for  $\text{C}_{2+}$  hydrocarbon formation as a function of  $\text{TiO}_x$  coverage.

Figure 8: Hydrogen partial pressure dependence for  $\text{C}_{2+}$  hydrocarbon formation as a function of  $\text{TiO}_x$  coverage.

Figure 9: CO partial pressure dependence for  $\text{C}_{2+}$  hydrocarbon formation as a function of  $\text{TiO}_x$  coverage.

Figure 10: A schematic for possible bonding between CO and peripheral  $\text{Ti}^{3+}$  sites.

Figure 11: A comparison between the predicted methanation rate and the experimental data as a function of  $\text{TiO}_x$  coverage. The solid line denotes the calculated rate for peripheral Rh sites active for both the  $\text{Ti}^{3+}$ -assisted reaction pathway and the normal reaction pathway on bare Rh. The dashed line represents the calculated

rate if the peripheral Rh sites only participate in the  $\text{Ti}^{3+}$ -assisted reaction pathway.

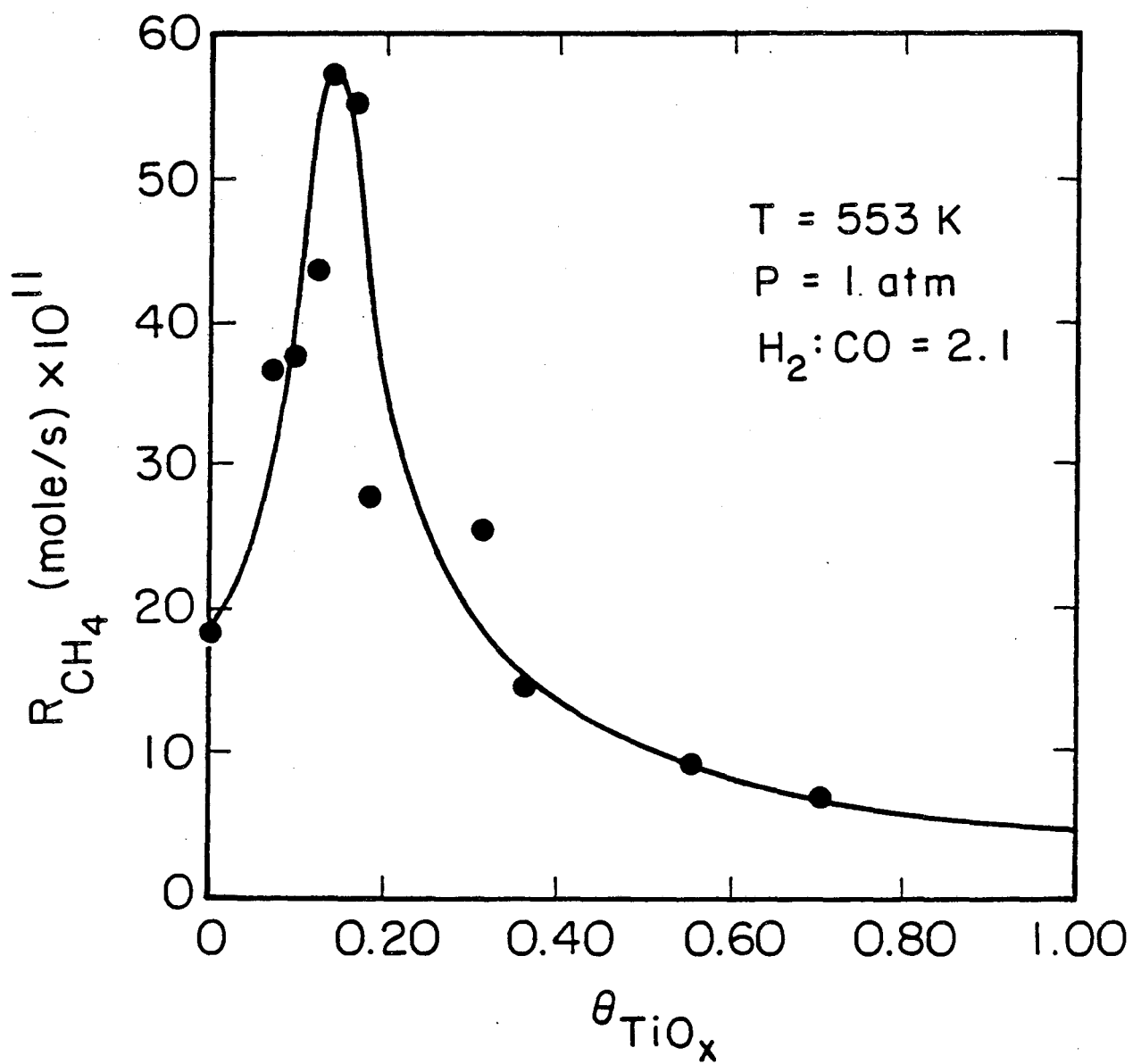


Figure 1

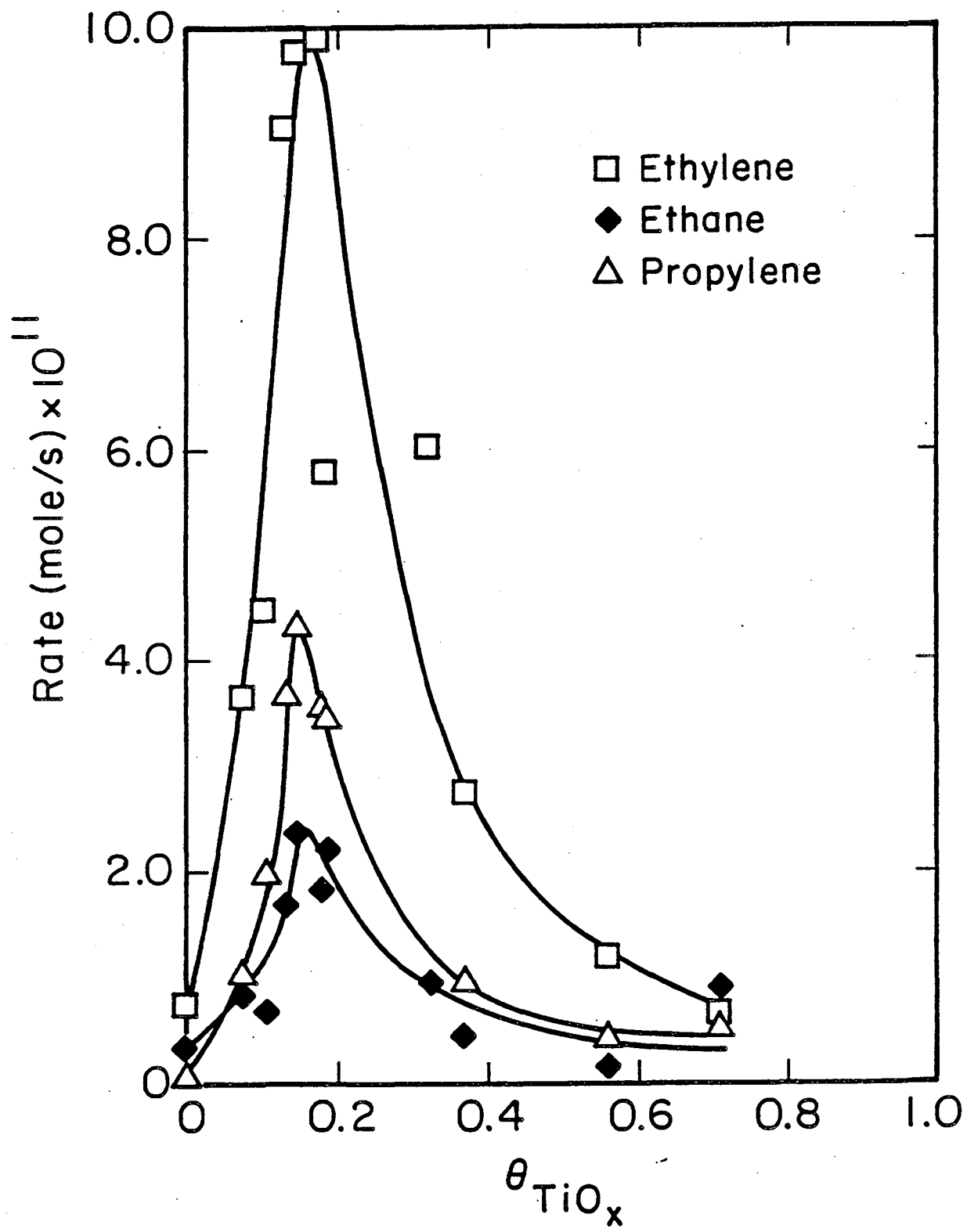


Figure 2

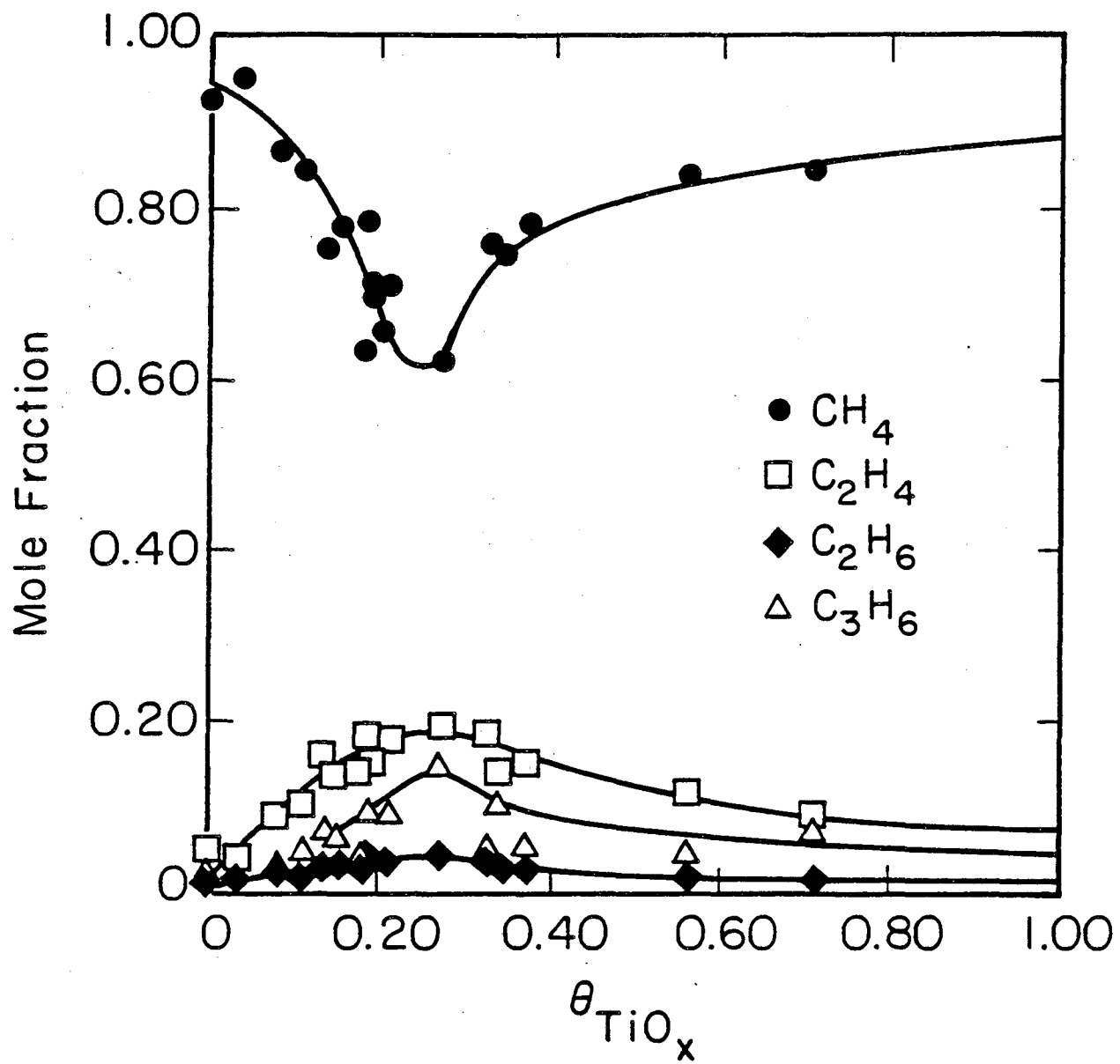


Figure 3

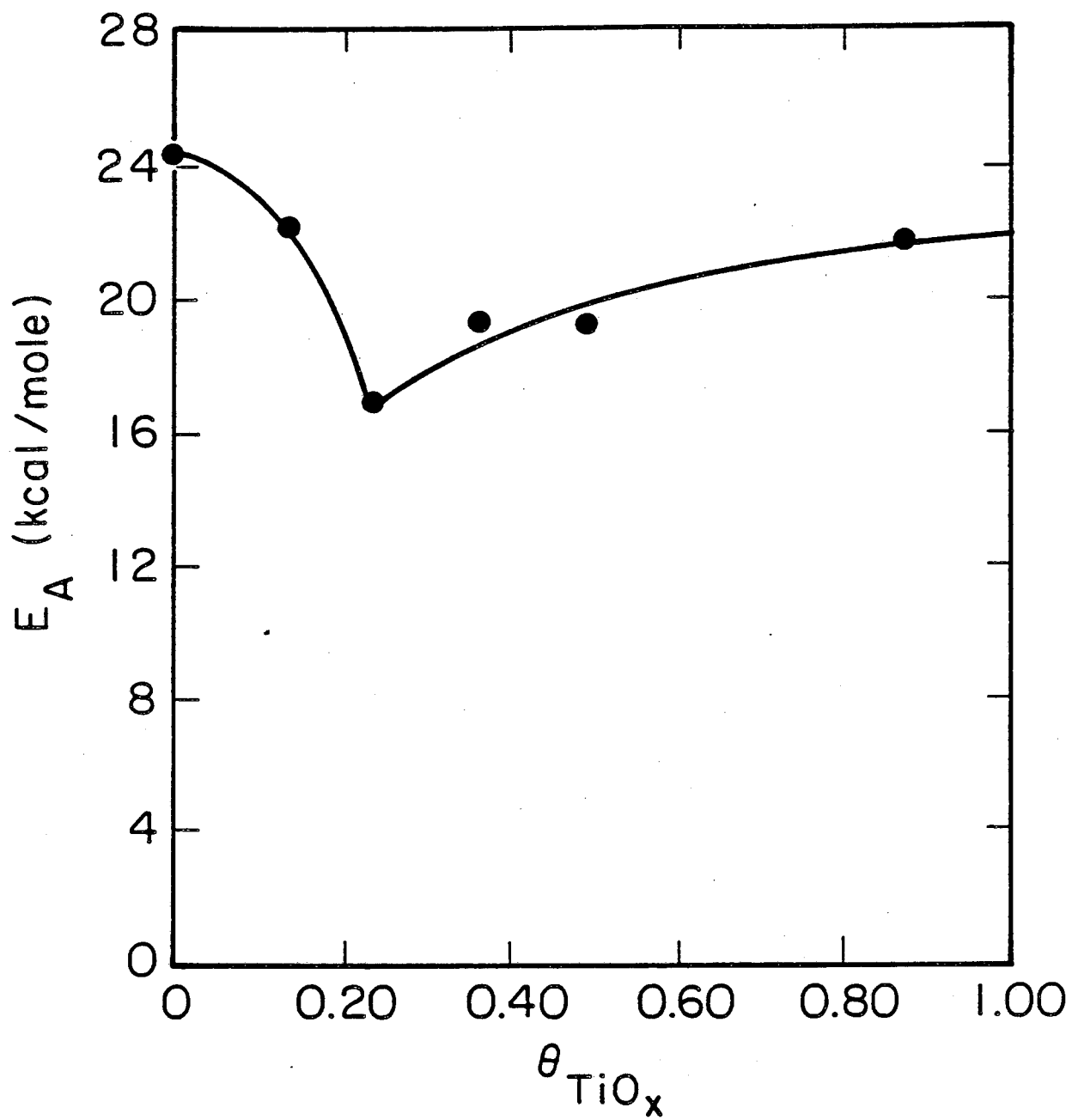


Figure 4



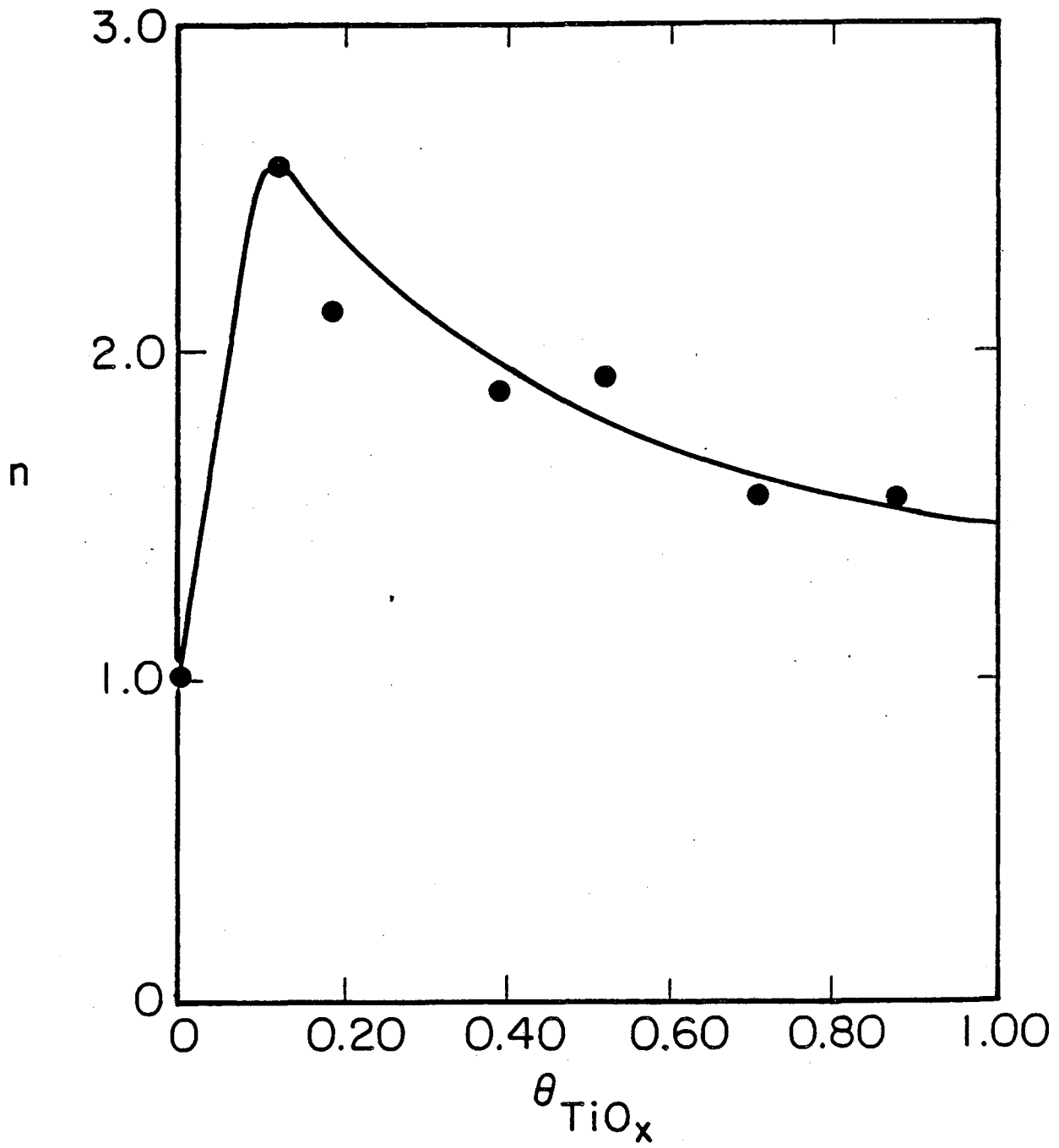


Figure 5

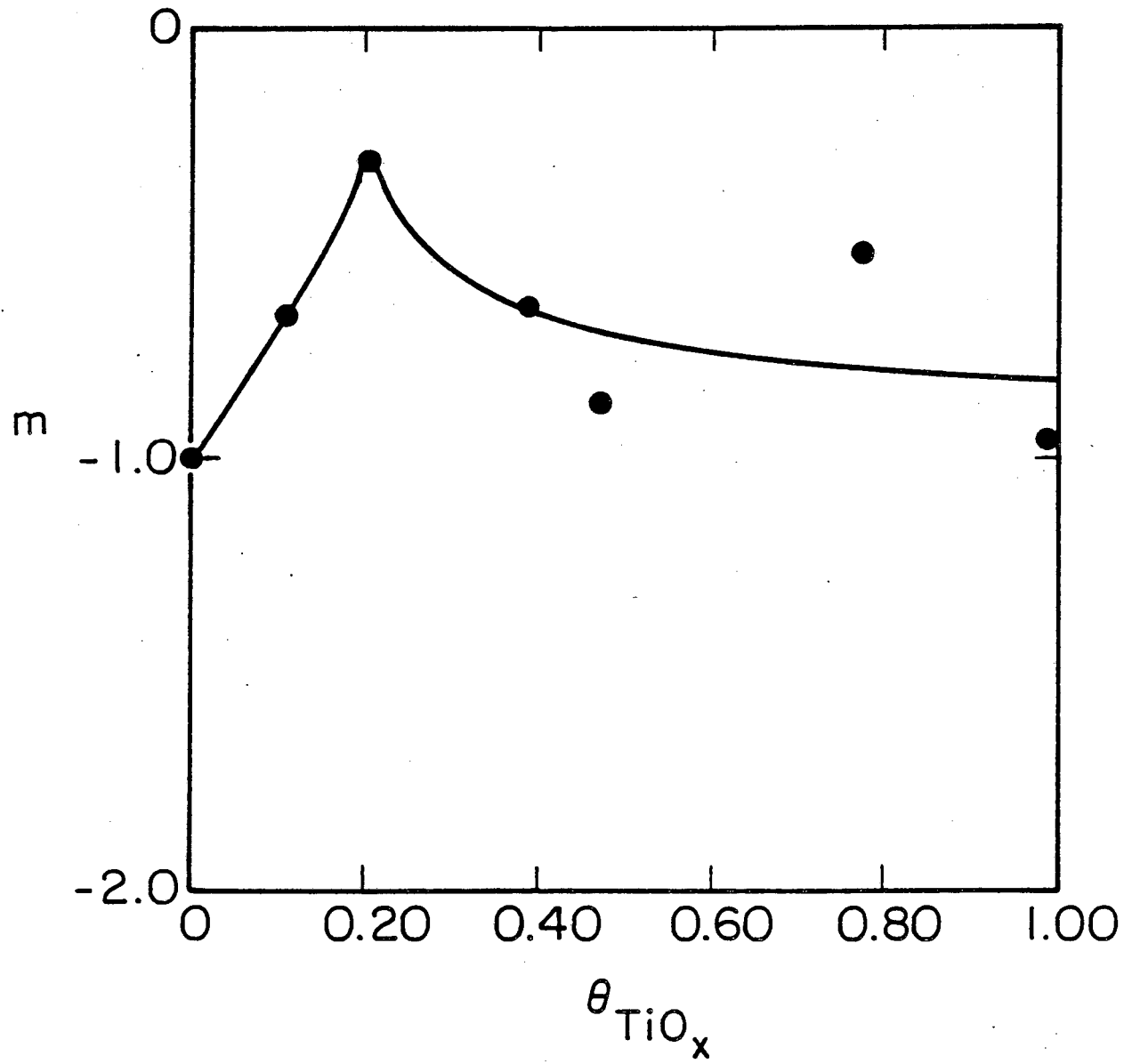


Figure 6

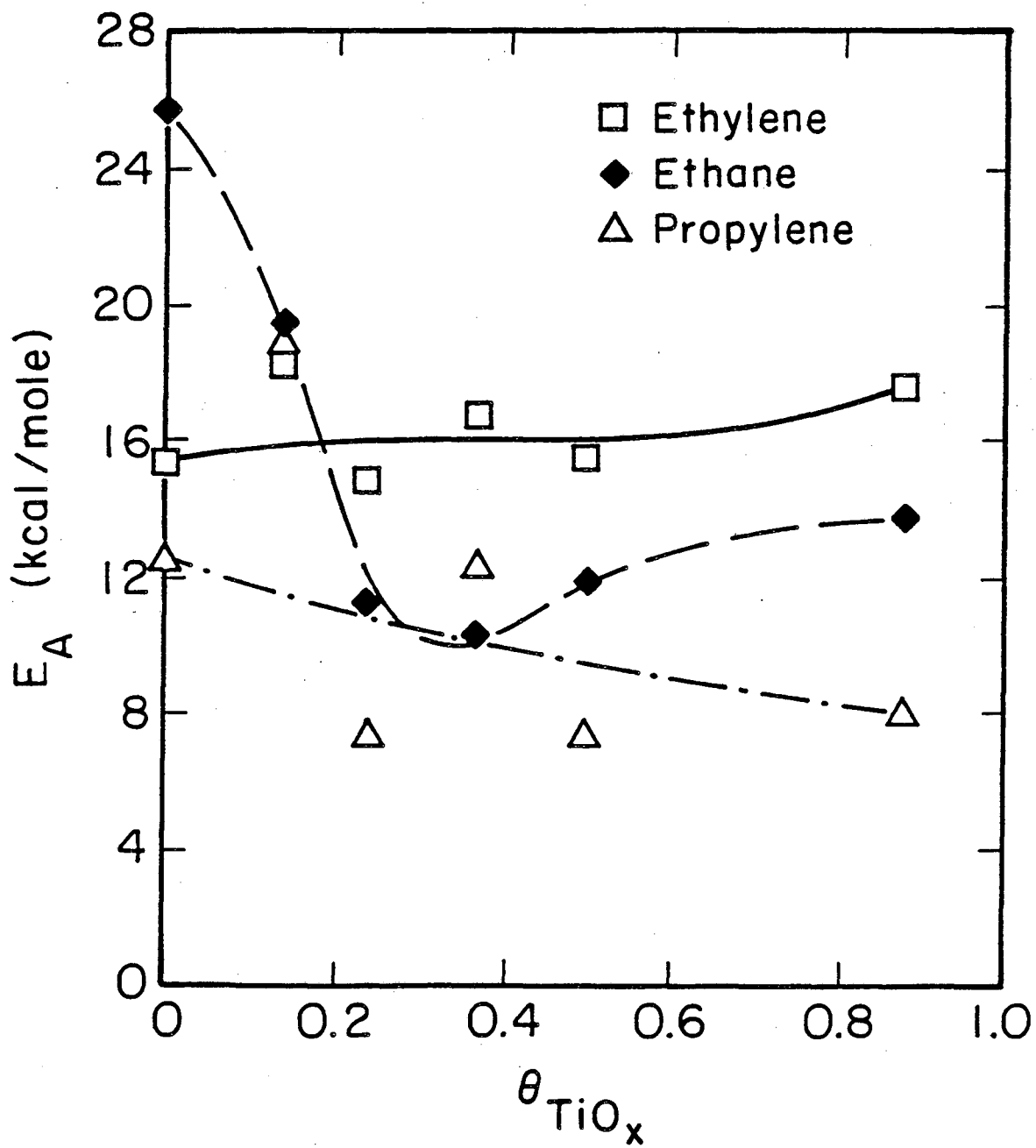


Figure 7

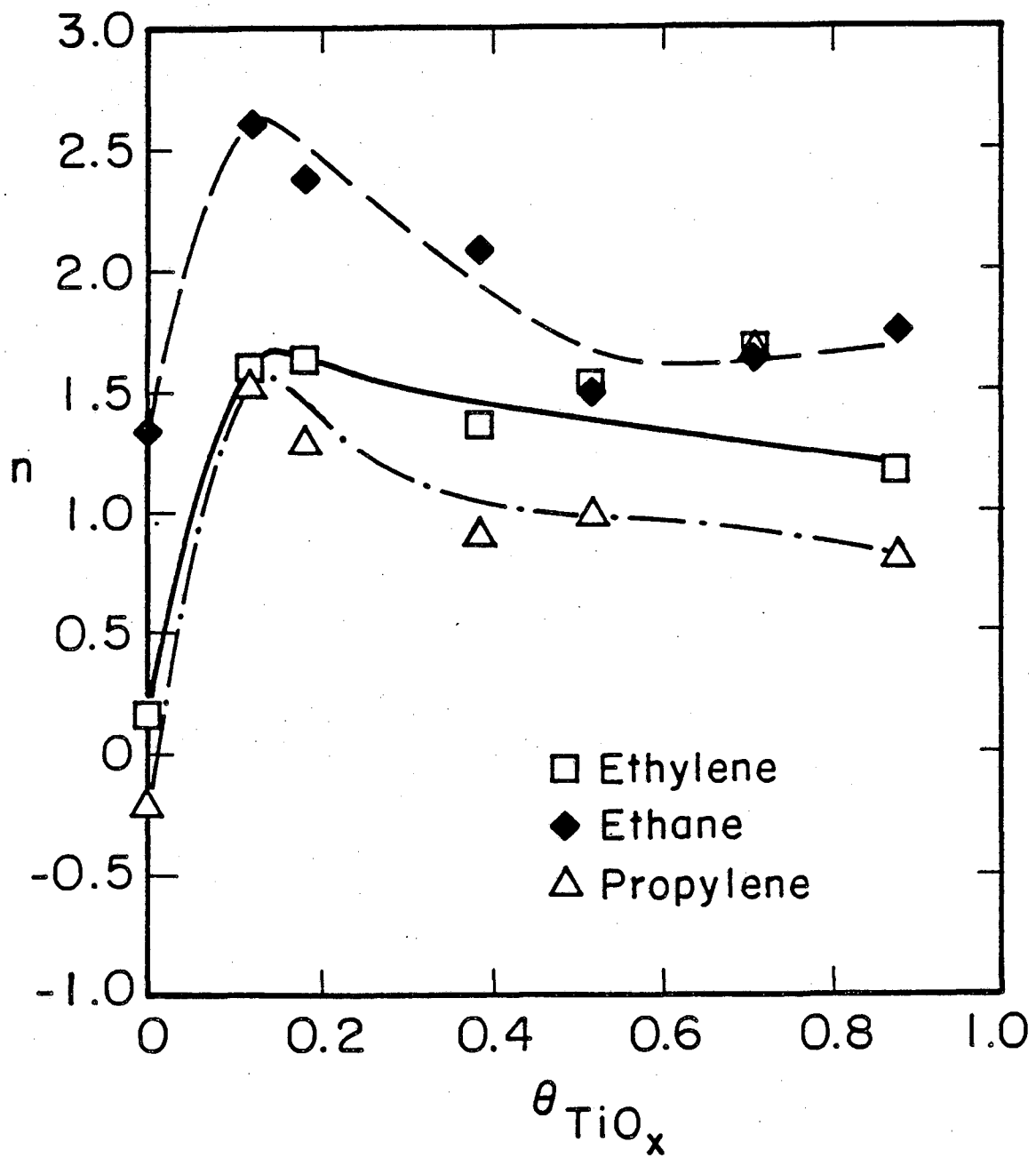


Figure 8

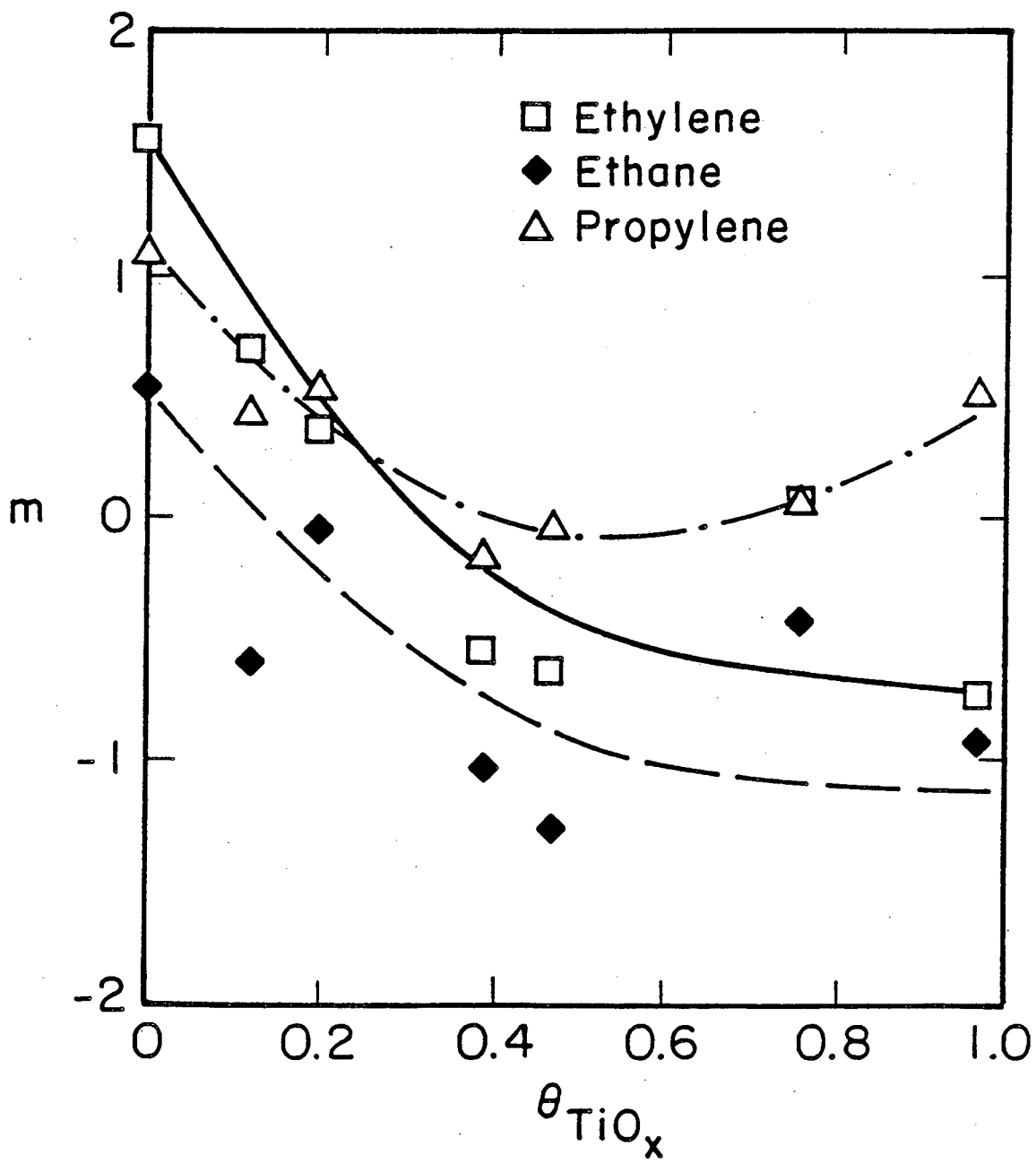


Figure 9

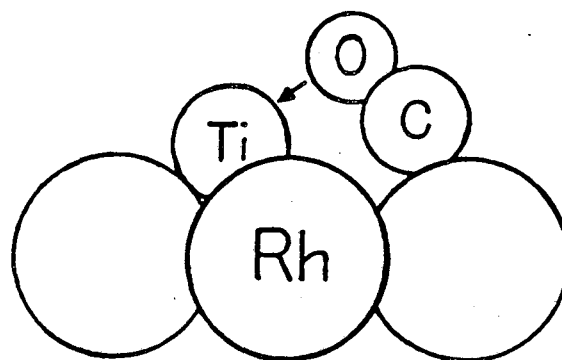
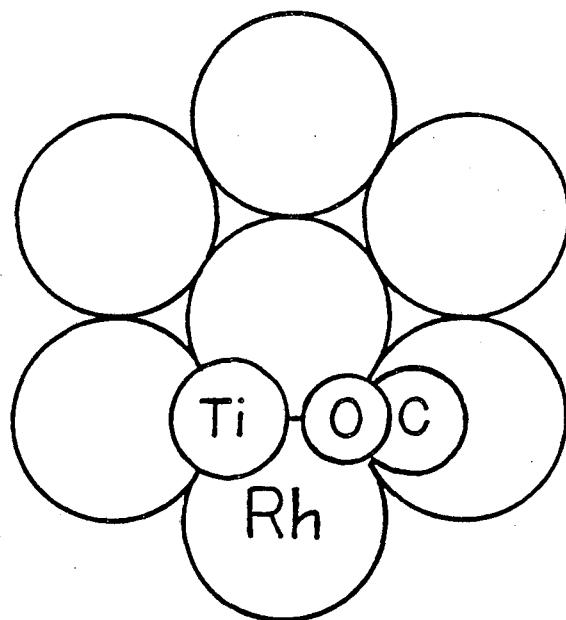


Figure 10

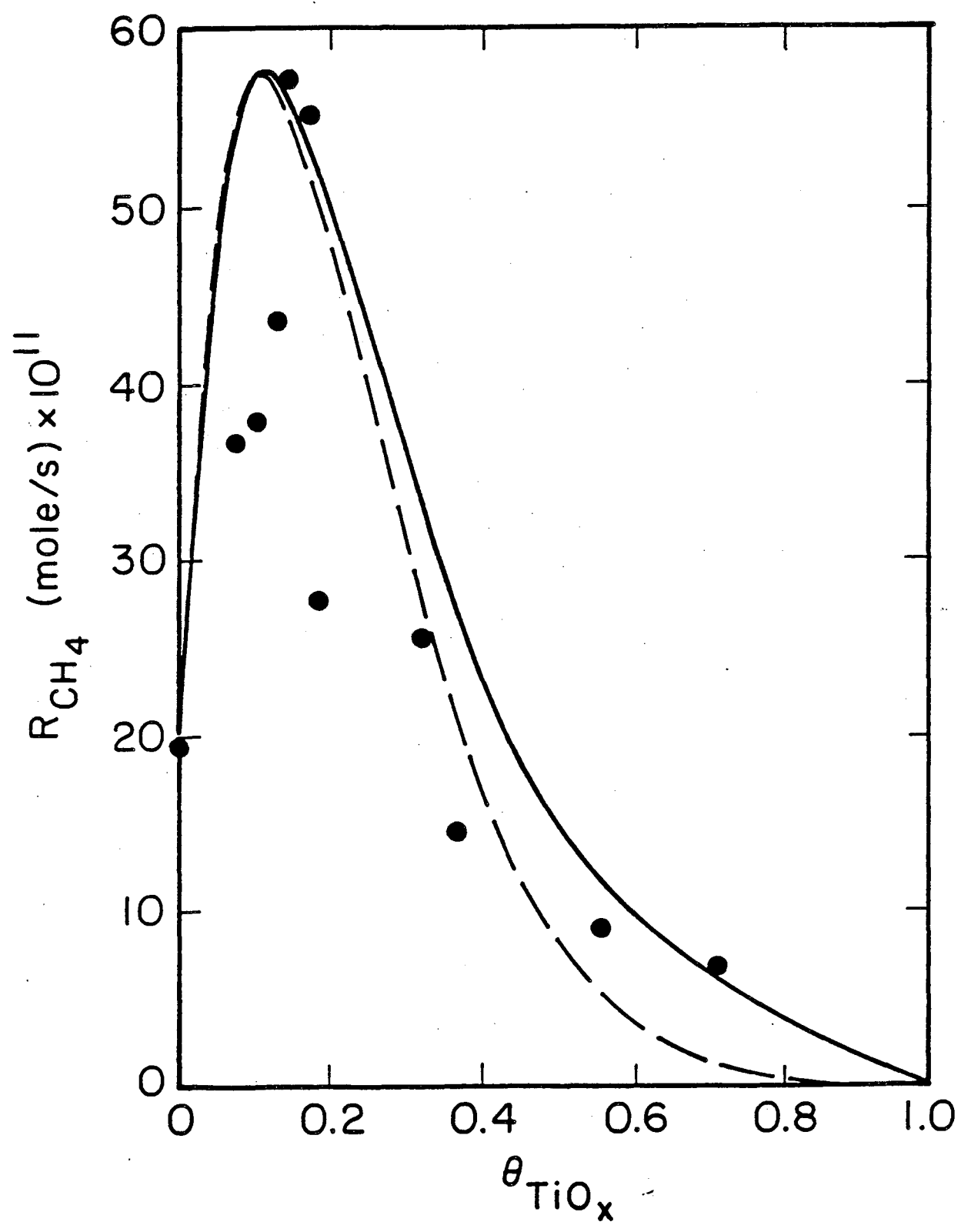


Figure 11

*LAWRENCE BERKELEY LABORATORY  
TECHNICAL INFORMATION DEPARTMENT  
UNIVERSITY OF CALIFORNIA  
BERKELEY, CALIFORNIA 94720*